European Journal of Pharmaceutics and Biopharmaceutics 77 (2011) 417–423

Contents lists available at ScienceDirect

European Journal of Pharmaceutics and Biopharmaceutics

journal homepage: www.elsevier.com/locate/ejpb

Research paper

Geometry and surface characteristics of gold nanoparticles influence their biodistribution and uptake by macrophages

Arnida [a,d], M.M. Janát-Amsbury [c,d], A. Ray [a,d], C.M. Peterson [c,d], H. Ghandehari [a,b,d,*]

[a] Department of Pharmaceutics and Pharmaceutical Chemistry, University of Utah, Salt Lake City, USA
[b] Department of Bioengineering, University of Utah, Salt Lake City, USA
[c] Department of Obstetrics and Gynecology, University of Utah, Salt Lake City, USA
[d] Center for Nanomedicine, Nano Institute of Utah, University of Utah, Salt Lake City, USA

ARTICLE INFO

Article history:
Available online 18 November 2010

Keywords:
Gold nanoparticles
Nanorods
Nanomedicine
Biodistribution
Ovarian tumor
Macrophages

ABSTRACT

Spherical and rod-shaped gold nanoparticles with surface poly(ethylene glycol) (PEG) chains were characterized for size, shape, charge, poly dispersity and surface plasmon resonance. The nanoparticles were injected intravenously to 6–8-week-old female nu/nu mice bearing orthotopic ovarian tumors, and their biodistribution in vital organs was compared. Gold nanorods were taken up to a lesser extent by the liver, had longer circulation time in the blood, and higher accumulation in the tumors, compared with their spherical counterparts. The cellular uptake of PEGylated gold nanoparticles by a murine macrophage-like cell line as a function of geometry was examined. Compared to nanospheres, PEGylated gold nanorods were taken up to a lesser extent by macrophages. These studies point to the importance of gold nanoparticle geometry and surface properties on transport across biological barriers.

1. Introduction

Advances in nanotechnology have led to the design and synthesis of organic and inorganic nanoconstructs with defined geometries, surface properties, conductivity and susceptibility to environmental stimuli such as heat and light. These constructs can take the form of nanotubes [1], nanorods [2], nanowires [3], nanocages [4], nanoshells [5], nanodisks [6] and a number of other geometries [7]. Reports are emerging that size, shape and surface properties play an important role in determining the cellular uptake and toxicity of nanoparticles in mammalian cells [8–10]. An area where nanoparticles are intensively used is in the treatment and/or diagnosis of cancers. Epithelial ovarian cancer (EOC) ranks as the sixth most common cancer in women worldwide and causes more deaths than any other type of female reproductive tract cancer [11]. Current standard therapy, cytoreductive surgery followed by chemotherapy based on the combination of a platinum derivative with a taxane, results in a complete response in 70% of EOC cases. However, most patients will eventually relapse within 18 months presenting with chemoresistant disease [12]. Acquisition of platinum-resistance is a major obstacle in the long-term survival of ovarian cancer patients and invites exploration of novel therapeutic alternatives that may overcome this barrier.

One class of inorganic particles that shows promise in targeted cancer therapy including ovarian cancer is gold nanoconstructs. Gold nanoparticles have been used to deliver antitumor agents such as tumor necrosis factor (TNF) or paclitaxel through the enhanced permeability and retention (EPR) effect [13]. The potential of gold nanoparticles to act as non-viral-based gene delivery systems has also been explored [14,15]. Physical and chemical properties of gold nanoparticles, in addition to their unique optical properties, make them particularly attractive for disease detection and therapy [16]. Gold nanoparticles with certain aspect ratios (e.g. rods) or compositions (spherical nanoshells) exposed to laser photoradiation can produce local heat that facilitates the destruction of diseased tissues such as solid tumors [17]. Previous studies have shown that size and surface chemistry of gold nanoparticles determine their biodistribution in non-tumor-bearing rats [18,19]. In this study, the surface of gold nanoparticles has been modified with poly (ethylene glycol) (PEG) to prolong their circulation time and facilitate functionalization among other attributes [20]. Such variations in geometry and surface properties can influence cellular uptake [21] and biodistribution. This differential uptake across biological barriers as a function of geometry and surface properties can be exploited for specific biomedical applications such as targeted therapy and/or diagnosis.

In this work, we have compared the biodistribution of commercially available PEGylated gold nanoparticles of similar size but

* Corresponding author. Department of Pharmaceutics and Pharmaceutical Chemistry, Nano Institute of Utah, University of Utah, 383 Colorow Road, Salt Lake City, UT 84108, USA. Tel.: +1 801 587 1566; fax: +1 801 585 0575.
E-mail address: hamid.ghandehari@pharm.utah.edu (H. Ghandehari).

0939-6411/$ - see front matter © 2010 Elsevier B.V. All rights reserved.
doi:10.1016/j.ejpb.2010.11.010

with varying shapes and surface charge in mice bearing orthotopic ovarian tumors as an *in vivo* EOC model. The EOC tumors were derived from human A2780 ovarian cancer cells, which were orthotopically inoculated into the ovarian bursa of female nude mice. Orthotopic implantation allows tumor cells to interact with ovarian stromal tissue and take advantage of the rich vascularization of the ovarian environment. Ovarian tumor formation and development are highly dependent upon angiogenesis, and the expression of pro-angiogenic factors such as vascular endothelial growth factor (VEGF) is increased in tumor development [22]. The ovarian microenvironment also allows for interaction with ovarian growth factors, signaling pathways and ECM molecules that affect tumor initiation, growth and progression. This approach recapitulates the clinical features of ovarian cancer and is thought to be a relevant EOC model. In addition to the *in vivo* biodistribution studies, the uptake of these nanoparticles by macrophages was evaluated.

2. Materials and methods

2.1. Preparation and characterization of nanoparticles

PEGylated gold nanoparticles (spherical particles of 50 nm in diameter and rod-shaped particles with reported dimensions of 10 × 45 nm) were purchased from Nanopartz, Inc. (Loveland, CO, USA). Before used, gold nanoparticle samples were incubated with cell culture medium for 1 week to evaluate for potential contaminations that adversely affect cells. Cytotoxicity was evaluated using WST-1 (4-[3-(4-Iodophenyl)-2-(4-nitrophenyl)-2H-5-tetrazolio]-1, 3-benzene disulfonate) assay to ensure that the particles were not toxic. Gold nanorods required a washing step to remove unbound and toxic cetyl trimethylammonium bromide (CTAB). They were centrifuged at 10,000 rpm for 30 min, the supernatant was subsequently removed and the resulting pellet was dissolved in phosphate-buffered saline (PBS) with a concentration that was adjusted to 20 μg/100 μL. The toxicity of the resulting samples was tested again *in vitro*. Spherical particles from stock solution were directly diluted in PBS to adjust the concentration to 30 μg/100 μL. Each batch of particles was characterized by UV–VIS spectrophotometry to determine their surface plasmon resonance (SPR) and optical density (OD). Inductive Coupled Plasma-Mass Spectrometry (ICP-MS) was used to determine gold concentration in each batch of nanoparticles. Transmission Electron Microscopy (TEM) was used to evaluate shape and size, Dynamic Light Scattering (DLS) for hydrodynamic volume and zeta potential for charge (Zetasizer Nano, Malvern Instrument Ltd., Worcestershire, UK). Measurements were done in triplicate except for size measurements with TEM (TECNAI F2 from Phillips, Hillsboro, OR, USA) where over 100 particles were measured (Table 1).

Table 1
Physicochemical characteristic of PEGylated gold nanoparticles.[a]

Property	Spheres	Rods
SPR peak (nm)	540	830
Reported size (nm)[b]	50	10 × 45
Size by TEM (nm)[c]	50 ± 1	10 × 45 ± 2X5
Shape discrepancy[d] (%)	0	6
Size by DLS (nm)[e]	88.85 ± 0.21	N/A
PDI	0.017 ± 0.001	N/A
Zeta potential (mV)	−27.1 ± 4.8	+1.13 ± 0.89

[a] All measurements were done in triplicate ± SD unless otherwise indicated.
[b] Reported by Nanopartz, Inc.
[c] TEM measurements were done for over 100 particles ± SD.
[d] Shape discrepancy refers to the presence of non-spheres or non-rod particles in sphere or rod samples measured by TEM. Zero percent discrepancy means all particles analyzed have the same shape.
[e] DLS measurement is not applicable for rod-shaped particles.

2.2. In vivo biodistribution in ovarian tumor-bearing mice

The animal model used to study the biodistribution of gold nanoparticles was the orthotopic A2780 human ovarian cancer. Six- to eight-week-old female nu/nu mice (strain code 088, homozygous) ordered from Charles River, Wilmington, MA, USA, were inoculated with 1,000,000 A2780 cells suspended in 10 μL PBS directly into the left ovarian bursa of each mouse. After 21–25 days of tumor growth, gold nanoparticles were injected intravenously (i.v.) via the tail vein. Three animals were assigned to study each time point (0, 30 min, 2 h, 6 h, 24 h and 1 week). Each mouse received 60 μg of spherical and 40 μg of rod nanoparticles per i.v. tail vein injection. Mice were sacrificed at predetermined time points at which blood, tumors and organs, including the contralateral, non-tumor-bearing ovary, were harvested for further analyses. Organ digestion method was followed with minor modification to evaluate organ gold content [23]. Briefly, each organ and blood sample was refluxed at 90 °C in 4 ml aqua regia for 24 h, followed by heating the samples at 130 °C for two hours until dried. Subsequently, samples were dissolved in 4 ml of 5% HNO_3. Before measurement with ICP-MS (ICP-MS; Agilent7500ce, Agilent Technologies Inc., Santa Clara, CA, USA), samples were diluted 200×. ICP-MS measurement was done with irradium as the internal standard.

2.3. In vitro uptake by murine macrophages

100,000 RAW264.7 cells (ATCC, Manassas, VA, USA) were plated on a 24-well plate and incubated under 5% CO_2 at 37 °C overnight. The next day, cells were incubated with 10 μg of gold nanoparticles. After 6 h incubation, the cells were washed three times with PBS to remove non-associated particles. They were subsequently lysed with 0.1 M NaOH and the amount of protein in each well was measured using bicinchoninic acid (BCA) protein assay kit (Micro BCA Protein Assay Kit, Thermo Scientific, Rockford, IL, USA). The lysates were digested three times with aqua-regia prior to measurement of gold content by ICP-MS. The uptake of particles was expressed by the amount of gold measured by ICP-MS normalized against protein weight. Experiments were done in triplicate. To evaluate the influence of serum proteins on cellular uptake, medium with reduced serum was used to incubate the cells with particles.

2.4. Protein binding assay

Gold nanoparticles at different gold concentrations (0–1.8 μg/ml) were mixed with 0.05 mg/ml bovine serum albumin (BSA). Intrinsic tryptophan fluorescence quenching induced by gold nanoparticles was recorded on Spectramax M2 from Molecular Device (Sunnyvale, CA, USA). Excitation was performed at 280 nm. The emission spectrum was recorded from 290 to 400 nm. The fluorescence quenching efficiency is defined as I^0/I, where I^0 and I are fluorescence intensity of BSA at peak in the absence and presence of gold nanoparticles respectively.

3. Results and discussion

3.1. Characterization

The physicochemical characteristics of the nanoparticles are outlined in Table 1 and representative TEM images are shown in Fig. 1. PEGylated gold nanoparticles (PEG M_w = 5000 Da) were chosen since non-PEGylated nanorods are toxic due to the presence of CTAB as a stabilizing agent. PEG is also known to improve the circulation half-life of particles and creates a steric shield, effectively

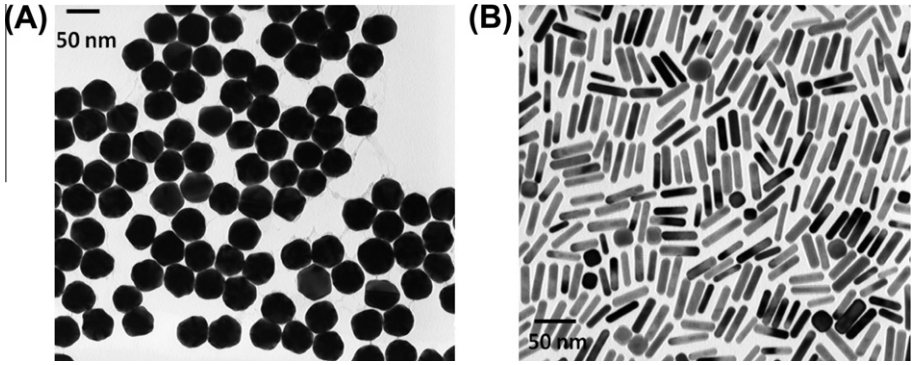

Fig. 1. Representative TEM images of PEGylated gold nanospheres (A) and rods (B). PEGylated gold nanospheres were uniform in size and shape, whereas there was 6% shape discrepancy for nanorods (See Table 1 for physicochemical characteristics of the particles).

preventing plasma proteins from adhering to the surface [24–27]. *In vitro* tests conducted suggest that particles remained in dispersion under physiological conditions. DLS showed one peak in the presence of serum proteins which was similar to the peak in the absence of serum. Further, UV–VIS spectra of particles confirmed lack of aggregation since no notable absorbance decrease was observed. The core size of the particles used was 50 nm in diameter for gold nanospheres and 10×45 nm for gold nanorods as reported by the manufacturer (Nanopartz, Loveland, CO, USA). Both types of gold nanoparticles were highly monodisperse in terms of size as measured by TEM and DLS while there was a 6% shape discrepancy for gold nanorods (Table 1). TEM was used to measure the core size of the particles in their dehydrated state while DLS provides the hydrodynamic diameter for particles. The difference in the TEM and DLS measurements is attributed to the hydrated PEG strands. Gold nanorods cannot be measured with DLS since the Stokes–Einstein equation for this measurement assumes a spherical shape in media. A poly dispersity index (PDI) was derived from the DLS measurements which represents the uniformity of the particle population in terms of their size. Spherical particles had a negative zeta potential value and nanorods were nearly neutral. The negative zeta potential of spherical particles was inherent and is thought to arise from citric acid used during the fabrication process. Attempts to remove the citric acid resulted in aggregation of the particles. The SPR peak frequency of metal nanoparticles has been shown to strongly depend on their size [28], shape [29], aggregation [30], structure (solid vs hollow) [31], as well as the dielectric properties of the surrounding media [32]. Spherical particles had an SPR peak at 540 nm which correlates to around 50 nm size in diameter. Gold nanorods had two SPR peaks, transverse and longitudinal, and their value listed herein (830 nm) is the longitudinal SPR.

Fig. 1 shows the representative TEM images of gold nanoparticles used in this study. Spherical gold nanoparticles were by and large very uniform in size and shape while there were several non-rod-shaped particles in the gold nanorod samples. This shape irregularity was quantified as shape discrepancy of roughly 6% (Table 1).

3.2. Biodistribution of gold nanoparticles in ovarian tumor-bearing mice

The *in vivo* fate of the nanoparticles and their transport across biological barriers by a particular administration route is determined by their physicochemical properties. In this work, the biodistribution of PEGylated gold nanoparticles of similar size (10×45 nm for rods and 50 nm diameters for spheres) but different geometries were evaluated in EOC-bearing mice.

It is known that nanoparticles can accumulate in solid tumors through the enhanced permeability and retention (EPR) effect [33]. Nanoparticles can also be cleared by macrophages of the reticuloendothelial system (RES), mainly Kupffer cells of the liver and to a lesser extent the macrophages of the spleen and the bone marrow [34–36].

The biodistribution of gold nanorods and spheres normalized to organ weight at different time points after injection were evaluated (Fig. 2). Both gold nanorods and the spherical particles were detected in all organs analyzed including the brain, however, the majority of uptake was observed in the liver and spleen. Comparative clearance of the nanoparticles in blood (Fig. 3A) show that between 30 min to 6 h post injection, gold nanorods were present at significantly higher concentrations compared to spherical particles. At 6 h, there were less than 1% of spherical particles per gram in the blood while 11% of nanorods remained. The ratio of area under the curve (AUC) between gold nanorods and gold nanospheres

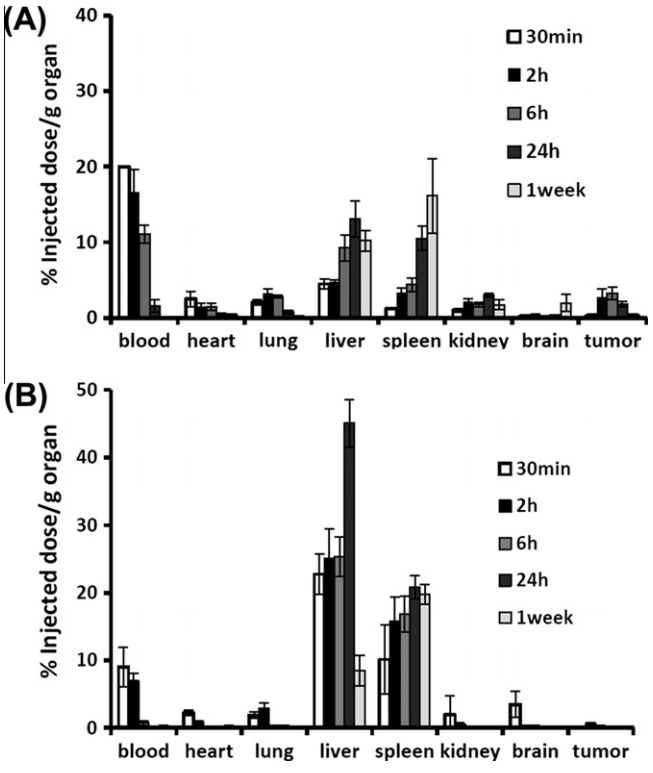

Fig. 2. Bioditribution of gold nanoparticles in non metastatic orthotropic ovarian tumor-bearing mice. (A) nanorods and (B) nanospheres. $n = 3 \pm$ SEM.

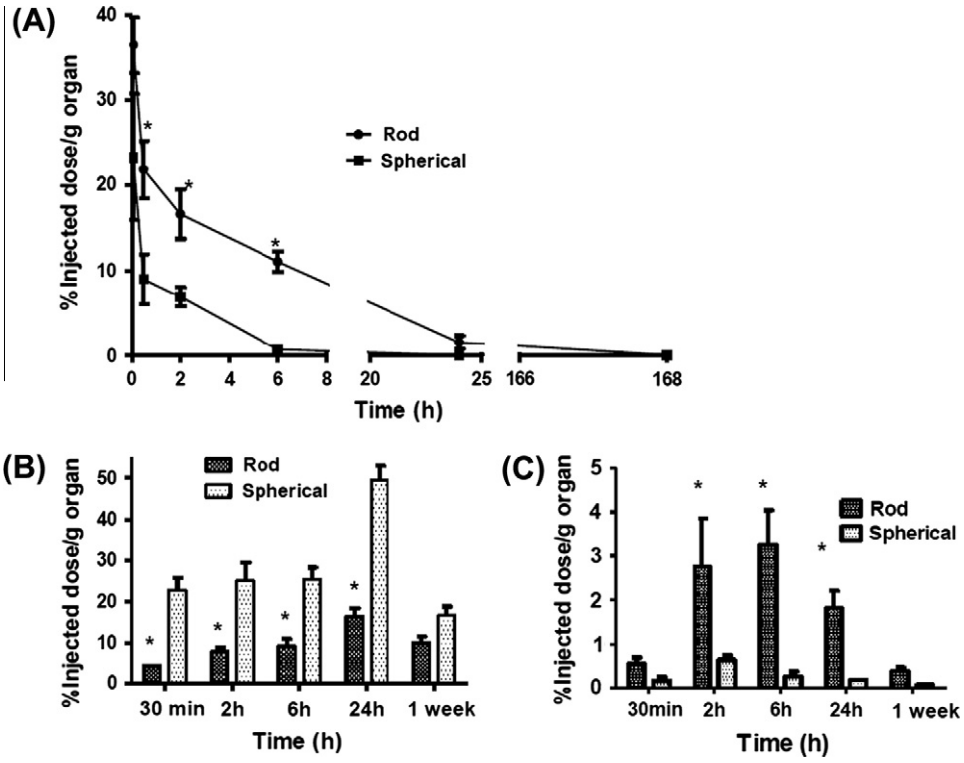

Fig. 3. Comparison of plasma profile (A), distribution in liver (B) and tumor (C) of rod and spherical particles as a function of time. $n = 3 \pm$ SEM. *Significant difference between rod and spherical particles $p < 0.05$.

was 4.1. This data clearly demonstrates that the circulation time of the PEGylated nanorods is higher than PEGylated gold nanospheres.

Accumulation of the particles in plasma, liver and tumor is shown in Fig. 3 as a function of time for both types of nanoparticles. Both spherical and rod-shaped particles continued to accumulate in the liver for up to 24 h. At 1 week time point, there was a notable decrease in the amount of gold detected in the liver suggesting clearance from this organ. The particles cleared may in part be excreted through the feces as we detected as much as 0.3% injected dose of gold per gram feces at the 1 week time point. The TEM images confirm this result where spherical and rod gold nanoparticles were observed in feces samples (data not shown).

When compared to nanorods, a notably higher extent of spherical particles was accumulated in the liver at all time points (Fig. 3B). Nanorods were taken up to a lower extent by the liver than spheres and circulated for a longer period of time in the blood (Fig. 3A) eventually resulting in a higher accumulation of the nanorods within tumor tissue (Fig. 3C). The average tumor weight was 5 g, hence as much as 15% of the injected nanorods accumulated in the tumor as shown at the 6 h time point. A combined effect of prolonged circulation time and a locally increased capillary permeability at the tumor site due to the EPR effect may be responsible for the increased accumulation of nanorods. It must also be noted that the spherical particles had a net negative charge, compared to nearly neutral rods. This charge effect, in addition to geometry, may also contribute to lower accumulation of the spheres in the tumors since it is known that negatively charged nanoparticles and macromolecular constructs are rapidly cleared from the blood stream [37].

3.3. In vitro uptake by macrophages

Macrophages are widely distributed in many tissues and clear from the body altered and senescent cells, invading particulates, as well as macromolecular ligands via a multitude of specialized plasma membrane receptors [38]. The propensity of macrophages to phagocytose foreign particles provides an opportunity for the efficient delivery of therapeutic agents to these cells [39]. However, in many tumor targeting scenarios, macrophages are not the target cell type, and phagocytosis by nontarget organs reduces the accumulation of the nanoparticles in the desired cell population. To partially explain the comparative *in vivo* biodistribution profile of the two types of nanoparticles under study, an *in vitro* experiment to evaluate their uptake by macrophages was carried out. Gold nanorods were taken up to a lesser extent by RAW 264.7 macrophages compared to spherical nanoparticles (Fig. 4). This observation in part explains the lower accumulation of rods in the liver compared to spheres and their longer circulation time in the blood.

Physicochemical properties such as nanoparticle size, surface charge and surface functionality influence particle uptake by macrophages. Particles bearing cationic or anionic surface charges have been shown to be subject to phagocytosis to a higher extent compared to neutral particles of the same size [40]. Hence, the increased uptake of the gold nanospheres can in part be due to its negative surface charge. In addition to surface charge, the shape of particles can play a role in the extent of phagocytosis by macrophages. For example oblong-shaped poly styrene-based microparticles exhibited higher attachment to the surface of macrophages compared to their spherical counterparts [41,42]. These and other studies [43–45] demonstrate that indeed shape of particles can be a factor in influencing their uptake by mammalian cells. Hence, in the present study, the influence of geometry of gold nanoparticles on their uptake by macrophages cannot be ruled out and further mechanistic studies can elucidate this effect.

3.4. Interaction of gold nanoparticles with bovine serum albumin

Serum proteins acting as opsonins are believed to contribute significantly to particle-macrophage association [46]. Adsorption

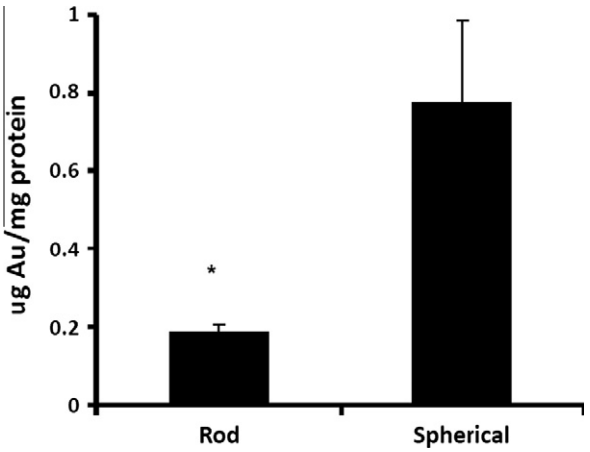

Fig. 4. Uptake of gold nanoparticles by RAW 264.7 macrophages expressed as the amount of gold detected by ICP-MS normalized to mg of protein. $n = 3 \pm SD$. *Significant difference between uptake of rod and spherical particles, $p < 0.01$.

of plasma proteins onto the surface of nanoparticles, known as opsonization, occurs the instant particles enter the blood stream [46]. Protein binding can increase the nanoparticle's effective size and change its surface charge which in turn can influence uptake by macrophages. Opsonization of nanoparticles is a crucial step by which they are recognized and cleared by cells of the mononuclear phagocyte system (MPS) [47]. To examine the influence of protein binding on cellular uptake, gold nanoparticles were incubated with bovine serum albumin as a model protein and their uptake by macrophages evaluated. Gold efficiently quenches the emission of many chromophores including tryptophan residues in proteins [48]. The efficiency of this quenching depends on the distance between the quencher and the protein [49]. The interaction of gold nanoparticles with BSA (Fig. 5) is presented as quenching efficiency which is the ratio between the fluorescence intensity of mixture of gold nanoparticles and BSA vs BSA alone. Spherical particles had a very strong quenching efficiency as shown in Fig. 5. In case of gold nanorods, however, there was little quenching even with increased concentration. This data suggests that BSA molecules interact strongly with spherical particles under study but not with nanorods.

This observation was confirmed with UV–VIS spectrum of gold nanoparticles where there was 4-nm red shift of surface plasmon resonance peak (SPR) for gold nanospheres in the presence of BSA while there was none for gold nanorods (data not shown). The red shift of gold nanoparticles' SPR represents the interaction of GNPs with other entities in close proximity. This result further confirms that despite the presence of PEGylated layers, gold nanospheres interact with serum albumin, while gold nanorods do not. The observed interactions can potentially be explained by the fact that the negatively charged spherical particles interact with the lysine residues on albumin molecules while nanorods, with a neutral charge have limited interaction with the protein.

The uptake of gold nanoparticles in the presence and absence of serum was compared. In the presence of serum, the uptake of gold nanospheres by macrophages was decreased; however, the relative uptake of nanorods was not significantly different with or without serum and was lower than their spherical counterparts (Fig. 6). The lack of differential uptake of gold nanorods in the absence and presence of serum is consistent with the observed limited interaction of these nanoparticles with BSA (Fig. 5). The reduced uptake of spherical particles in the presence of serum suggests that their uptake is opsonin-independent and is probably through direct recognition by scavenger receptors. It is known that scavenger receptors recognize anionic particles and facilitate uptake by the RES [50–52]. Negatively charged spherical particles can potentially bind to available cationic sites on the macrophage surface and be recognized by scavenger receptors while adsorption of proteins on their surface may alter their overall charge, prevent such interaction and result in fewer uptake. It must be noted, however, that the zeta potential of protein-bound spherical particles is only slightly negative at −6.1 mV, and hence in addition to the influence of surface charge, nanoparticle geometry has probably played a role in the cellular uptake and biodistribution of the particles under study.

In the present study, we used commercially available gold nanoparticles. Further tailor-made synthesis of colloidally stable gold nanoparticles with identical surface properties but different geometries, as well as mechanistic studies to evaluate the influence of shape, can shed light into the potential influence of gold nanoparticle geometry on cellular uptake and *in vivo* biodistribution. Another important factor that needs to be considered is that blood in the circulation is in rapid flow and is constantly sheared. Hence, *in vivo* interaction of particles with phagocytic cells is under fluid dynamics rather than under static conditions [53]. The relative orientation of rod nanoparticles in the blood may also yet be another factor in minimizing phagocytosis and maximizing the EPR effect and uptake by the ovarian tumors. The influence of

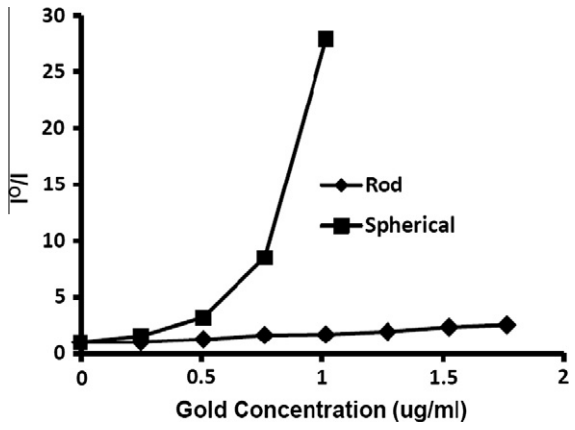

Fig. 5. Interaction between gold nanoparticles with bovine serum albumin expressed as quenching efficiency (I^0/I), where I^0 and I are fluorescence in the absence and presence of gold nanoparticles.

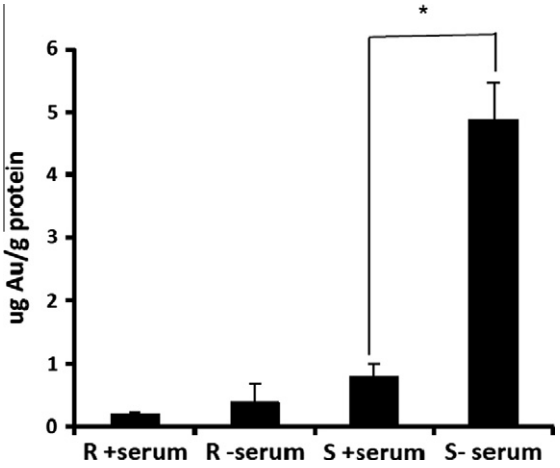

Fig. 6. Comparison of uptake of gold nanoparticles by RAW 264.7 macrophages in the presence and absence of serum expressed as the amount of gold detected by ICP-MS normalized to mg of protein. R = rod; S = spherical; $n = 3 \pm SD$, $^*p < 0.01$.

geometry of nanoparticles on transport in the blood stream and penetration across endothelial barriers is another area that needs detailed investigation.

4. Conclusions

The biodistribution of PEGylated gold nanorods and spheres of similar size, but different shapes and surface charge was evaluated in orthotopic EOC-bearing mice. Both nanoparticles accumulated to a significant extent in the liver and spleen. In all other organs studied, gold nanorods accumulated to a significantly higher extent compared to nanospheres. Rod-shaped nanoparticles had a longer circulation time in the blood and preferentially accumulated in solid tumors to a higher extent compared to spherical nanoparticles. Gold nanorods were taken up by macrophages *in vitro* to a lesser extent compared to nanospheres. The mechanism of phagocytosis of these nanoparticles appears to be opsonin-independent since particles were recognized by the macrophages probably through the scavenger receptors. These results have implications in the *in vitro* and *in vivo* biomedical applications of gold nanoparticles. The details of the potential mechanism(s) of the differential biodistribution and cellular uptake of gold nanorods vs spheres needs further investigation.

Acknowledgements

We thank Yong En Sun, Shraddha Sadekar, and Erin Soisson for their assistance in animal surgery and tissue harvesting. Financial support was provided by the National Institutes of Health (R01 DE019050), the Utah Science Technology and Research (USTAR) initiative and a Catalyst Grant from the University of Utah Health Sciences Center.

Appendix A. Supplementary material

Supplementary data associated with this article can be found, in the online version, at doi:10.1016/j.ejpb.2010.11.010.

References

[1] Y. Choi, L.A. Baker, H. Hillebrenner, C.R. Martin, Biosensing with conically shaped nanopores and nanotubes, Phys. Chem. Chem. Phys. 8 (2006) 4976–4988.
[2] S. Giri, B.G. Trewyn, M.P. Stellmaker, V.S.Y. Lin, Stimuli-responsive controlled-release delivery system based on mesoporous silica nanorods capped with magnetic nanoparticles, Angew. Chem. Int. Ed. 44 (2005) 5038–5044.
[3] M. Ferrari, Cancer nanotechnology: opportunities and challenges, Nat. Rev. Cancer 5 (2005) 161–171.
[4] J. Chen, B. Wiley, Z.Y. Li, D. Campbell, F. Saeki, H. Cang, L. Au, J. Lee, X. Li, Y. Xia, Gold nanocages; engineering their structure for biomedical applications, Adv. Mater. 17 (2005) 2255–2261.
[5] L.R. Hirsch, R.J. Stafford, J.A. Bankson, B. Rivera, R.E. Price, J.D. Hazle, N.J. Halas, J.L. West, Nanoshell-mediated near-infrared thermal therapy of tumors under magnetic resonance guidance, Proc. Natl. Acad. Sci. 100 (2003) 13549–13554.
[6] R.O. Ryan, Nanodisk: hydrophobic drug delivery vehicles, Expert Opin. Drug Deliv. 5 (2008) 343–351.
[7] V. Torchilin, Multifunctional and stimuli-sensitive pharmaceutical nanocarriers, Eur. J. Pharm. Biopharm. 71 (2009) 431–444.
[8] B.D. Chithrani, A.A. Ghazani, W.C.W. Chan, Determining the size and shape dependence of gold nanoparticle uptake into mammalian cells, Nanoletters 6 (2006) 662–668.
[9] .Y.S. Chen, Y.C. Hung, I. Liau, G.S. Huang, Assessment of the in vivo toxicity of gold nanoparticles, Nanoscale Res. Lett. 4 (2009) 858–864.
[10] A. Nan, X. Bai, S.J. Son, S.B. Lee, H. Ghandehari, Cellular uptake and cytotoxicity of silica nanotubes, Nano Lett. 8 (2008) 2150–2154.
[11] D.M. Parkin, F. Bray, J. Ferlay, P. Pisani, Global cancer statistics, 2002, CA Cancer J. Clin. 55 (2005) 74–108.
[12] R.F. Ozols, Treatment goals in ovarian cancer, Int. J. Gynecol. Cancer 15 (2005) 3–11.
[13] G.F. Paciotti, L. Myer, D. Weinreich, D. Goia, N. Pavel, R.E. McLaughlin, L. Tamarkin, Colloidal gold; a novel nanoparticle vector for tumor directed drug delivery, Drug Deliv. 11 (2004) 169–183.
[14] M. Thomas, A.M. Klibanov, Conjugation to gold nanoparticles enhances polyethylenimine's transfer of plasmid DNA into mammalian cells, Proc. Natl. Acad. Sci. 100 (2003) 9138–9143.
[15] A.K. Salem, P.C. Searson, K.W. Leong, Multifunctional nanorods for gene delivery, Nat. Mater. 2 (2003) 668–671.
[16] P.K. Jain, I.H. El-Sayed, M.A. El-Sayed, Au nanoparticles target cancer, Nanotoday 2 (2007) 18–29.
[17] X. Huang, P.K. Jain, I.H. El-Sayed, M.A. El-Sayed, Gold nanoparticles: interesting optical properties and recent applications in cancer diagnostics and therapy, Nanomedicine 5 (2007) 681–693.
[18] M. Semmler-Behnke, W.G. Kreyling, J. Lipka, S. Fertsch, A. Wenk, S. Takenaka, G. Schmid, W. Brandau, Biodistribution of 1. 4-and 18-nm gold particles in rats, Small 4 (2008) 108–2111.
[19] J. Lipka, M. Semmler-Behnke, R.A. Sperling, A. Wenk, S. Takenaka, C. Schleh, T. Kissel, W.J. Parak, W.G. Kreyling, Biodistribution of PEG-modified gold nanoparticles following intratracheal instillation and intravenous injection, Biomaterials 31 (2010) 6574–6581.
[20] L.E. Vlerken, T.K. Vyas, M.M. Amiji, Poly(ethylene glycol)-modified nanocarriers for tumor-targeted and intracellular delivery, Pharm. Res. 24 (2007) 1405–1414.
[21] Arnida, A. Malugin, H. Ghandehari, Cellular uptake and toxicity of gold nanoparticles in prostate cancer cells: a comparative study of rods and spheres, J. Appl. Toxicol. 30 (2010) 212–217.
[22] S. Inan, S. Vatansever, C. Celik-Ozenci, M. Sanci, N. Dicle, R. Demir, Immunolocalizations of VEGF, its receptors flt-1, KDR and TGF-beta's in epithelial ovarian tumors, Histol. Histopathol. 21 (2006) 1055–1064.
[23] Y. Akiyama, T. Mori, Y. Katayama, T. Niidome, The effect of PEG grafting level and injection dose on gold nanorod biodistribution in the tumor-bearing mice, J. Control. Release 139 (2009) 81–84.
[24] M. Yokoyama, T. Okano, Y. Sakurai, H. Ekimoto, C. Shibazaki, K. Kataoka, Toxicity and antitumor activity against solid tumors of micelle-forming polymeric anticancer drug and its extremely long circulation in blood, Cancer Res. 51 (1991) 3229–3236.
[25] T. Niidome, M. Yamagata, Y. Okamoto, Y. Akiyama, H. Takahashi, T. Kawano, Y. Katayama, Y. Niidome, PEG-modified gold nanorods with a stealth character for in vivo application, J. Control. Release 114 (2006) 343–347.
[26] S.M. Moghimi, C.J.H. Porter, I.S. Muir, L. Illum, S.S. Davis, Non-phagocytic uptake of intravenously injected microsphere in rat spleen; influence of particle size and hydrophilic coating, Biochem. Biophys. Res. Commun. 177 (1991) 861–866.
[27] J.M. Harris, Poly(ethylene glycol) Chemistry: Biotechnical and Biomedical Applications, Plenum Press, New York, 1992.
[28] U. Kreibig, L. Genzel, Optical absorption of small metallic particles, Surf. Sci. 156 (1985) 678–700.
[29] D. Sarkar, N.J. Halas, General vector basis function solution of Maxwell's equations, Phys. Rev. E 56 (1997) 1102–1112.
[30] J.P. Novak, D.L. Feldheim, Assembly of phenylacetylene-bridged silver and gold nanoparticle arrays, J. Am. Chem. Soc. 122 (2000) 3979–3980.
[31] Y. Sun, Y. Xia, Increased sensitivity of surface plasmon resonance of gold nanoshells compared to that of gold solid colloids in response to environmental changes, Anal. Chem. 74 (2002) 5297–5305.
[32] C.L. Haynes, R.P. Van Duyne, Nanosphere lithography: a versatile nanofabrication tool for studies of size-dependent nanoparticle optics, J. Phys. Chem. B 105 (2001) 5599–5611.
[33] H. Maeda, J. Wu, T. Sawa, Y. Matsumura, Tumor vascular permeability and the EPR effect in macromolecular therapeutics: a review, J. Control. Release 65 (2000) 271–284.
[34] G. Gregoriadis, Observations on entrapped solute retention, vesicle clearance and tissue distribution in vivo, in: G. Gregoriadis (Ed.), Liposomes as drug carriers: recent trends and progress, Wiley, New York, 1998, pp. 3–11.
[35] L. Illum, S.S. Davis, The organ uptake of intravenously administered colloidal particles can be altered using a non-ionic surfactant (poloxamer 338), FEBS Lett. 167 (1984) 79–84.
[36] S.M. Moghimi, S.S. Davis, Innovations in avoiding particle clearance from blood by Kupffer cells: cause for reflection, Crit. Rev. Ther. Drug Carr. Syst. 11 (1994) 1089–1106.
[37] T.S. Levchenko, R. Rammohan, A.N. Lukyanov, K.R. Whiteman, V.P. Torchilin, Liposome clearance in mice: the effect of a separate and combined presence of surface charge and polymer coating, Int. J. Pharm. 240 (2002) 95–102.
[38] S. Gordon, The macrophage, Bioessay 17 (1995) 977–986.
[39] M.J. Poznansky, R.L. Juliano, Biological approaches to the controlled delivery of drugs: a critical review, Pharmacol. Rev. 36 277 (1985) 277–287.
[40] T. Lars, M. Hans, W. Elke, Phagocytosis and phagosomal fate of surface-modified microparticles in dendritic cells and macrophages, Pharm. Res. 20 (2003) 221–228.
[41] J.A. Champion, S. Mitragotri, Shape induced inhibition of phagocytosis of polymer particles, Pharm. Res. 26 (2009) 244–249.
[42] J.A. Champion, S. Mitragotri, Role of target geometry in phagocytosis, Proc. Natl. Acad. Sci. 103 (2006) 4930–4934.
[43] X. Huang, X. Teng, D. Chen, F. Tang, J. He, The effect of the shape of mesoporous silica nanoparticles on cellular uptake and cell function, Biomaterials 31 (2010) 438–448.
[44] D. Chithrani, A.A. Ghazani, W.C.W. Chan, Determining the size and shape dependence of gold nanoparticle uptake into mammalian cells, Nanoletters 6 (2006) 662–668.
[45] F.E. Alemdaroglu, N.C. Alemdaroglu, P. Langguth, A. Herrmann, Cellular uptake of DNA block copolymer micelles with different shapes, Macromol. Rapid Commun. 29 (2008) @@nbsp;326–329.
[46] D.E. Owend, N.A. Peppas, Opsonization biodistribution and pharmacokinetics of polymeric nanoparticles, Int. J. Pharm. 307 (2006) 93–102.

[47] J.W.B. Bradfield, in: S.S. Davis, L. Illum, J.G. McVie, E. Tomlinson (Eds.), Microspheres in drug therapy, Elsevier, Amsterdam, 1984, pp. 25–37.
[48] S.H. Brewer, W.R. Glomm, M.C. Johnson, M.K. Knag, S. Franzen, Probing BSA binding to citrate-coated gold nanoparticles and surfaces, Langmuir 21 (2005) 9303–9307.
[49] M.G. Sandros, D. Gao, C. Gokdemir, D.E. Benson, General high affinity approach for the synthesis of fluorophore appended protein nanoparticle assemblies, Chem. Commun. 22 (2005) 2832–2834.
[50] Y. Takakura, T. Fujita, H. Furitsu, M. Nishikawa, H. Sezaki, M. Hashida, Pharmacokinetics of succinylated proteins and dextran sulfate in mice: implications for hepatic targeting of protein drugs by direct succinylation via scavenger receptors, Int. J. Pharm. 105 (1994) 19–29.
[51] R.W. Jansen, G. Molema, G. Harms, J.K. Kruijt, T.J.C. van Berkel, M.J. Hardonk, D.K.F. Meijer, Formaldehyde treated albumin contains monomeric and polymeric forms that are differently cleared by endothelial and Kupffer cells of the liver: evidence for scavenger receptor heterogeneity, Biochem. Biophys. Res. Commun. 180 (1991) 23–32.
[52] A. Rigotti, S.L. Acton, M. Krieger, The class B scavenger receptors SR-BI and CD36 are receptors for anionic phospholipids, J. Biol. Chem. 270 (1995) 16221–16224.
[53] Y. Geng, P. Dalhaimer, S. Cai, R. Tsai, M. Tewari, T. Minko, D.E. Discher, Shape effects of filaments versus spherical particles in flow and drug delivery, Nat. Nanotechnol. 2 (2007) 249–255.